NUSANTARA BIOSCIENCE
Vol. 9, No. 3, pp. 251-259
August 2017

ISSN: 2087-3948
E-ISSN: 2087-3956
DOI: 10.13057/nusbiosci/n090303

Assessment of the successfulness of mangrove plantation program through the use of open source software and freely available satellite images

ILYAS NURSAMSI[1,♥], WULAN RATNA KOMALA[2]

[1]Bird Conservation Society (BICONS). Bandung 40184, West Java, Indonesia.♥email: ilyasnursyamsi05@gmail.com
[2]Department of Biology, Faculty of Mathematics and Natural Sciences, Universitas Padjadjaran. Jatinangor, Sumedang 45363, West Java, Indonesia.

Manuscript received: 10 May 2016. Revision accepted: 13 June 2017.

Abstract. *Nursamsi I, Komala WR.2017. Assessment of the successfulness of mangrove plantation program through the use of open source software and freely available satellite images. Nusantara Bioscience 9: 251-259.* Mangrove forest has a major role in the process of human-environment interaction, but almost every mangrove forest in the world is under threat. In Indonesia alone, 25% of South East Asia's mangroves are at a risk. The continued decline in mangrove forest induced by anthropogenic activity has made all the stakeholders who have the concern at the mangrove forest preservation worried, including the government. There were several programs have been performed by the government to preserve the mangrove forest. One of the programs was "Mangrove Rehabilitation Program in three districts: Ciamis, Indramayu, and Subang" held by Forestry Department of West Java Province in 2007. The aims of this study were to assess the changes in mangrove forest area before the program performed and to evaluate the successfulness of the program, using the increasing of mangrove forest area as a parameter. This study was conducted only in Subang and Indramayu Districts of West Java, Indonesia. The assessment was conducted using Landsat 4-5 TM, Landsat 7 ETM+, and Landsat 8 OLI acquired in 1996, 2006, and 2016 respectively. For each image, a supervised classification method was performed using open source GRASS GIS software. The resulting maps were then compared to quantify the changes. Field work activity conducted and confirmed the changes that occurred in the study areas. Our study shows that all of the two districts exhibit successfulness of the plantation program. Ground truth survey confirmed that the successfulness of the plantation program is due to the participation of communities in the area of study. This study also shows that by using open source software and freely available satellite images, the fast, robust, and reliable data as an initial step to monitor both short-term and long-term plantation program can be collected effectively and inexpensively.

Keywords: Classification, Indramayu, Landsat TM/ETM+/OLI, mangroves, remote sensing, Subang

Abbreviations: TM = Thematic Mapper, ETM+ = Enhanced Thematic Mapper, OLI = Operational Land Imagery, DN = Digital Number

INTRODUCTION

Mangroves are coastal forests found in sheltered estuaries and along river banks and lagoons in the tropics and subtropics. The term 'mangrove' describes both the ecosystem and the plant families that have developed specialized adaptations living in this tidal environmental (FAO 2007). Mangrove forest ecosystems fulfill some of important functions in terms of providing wood and non-wood forest products (Hussain and Badola 2010), coastal protection (Alongi 2008), conservation of biological diversity and provision of habitat (Barbier et al. 2011), spawning grounds and nutrients for a variety of fish and shellfish (FAO 2007).

The total area of mangroves in the year 2011 approximately were 10,872,000 ha spread in 118 countries (IUCN I-IV). Indonesia is the country with the largest extent of mangrove in the world amounted to 3,112,989 ha, representing 22.6% of the world's total mangrove ecosystems (Giri et al. 2011). On the basis of FAO data, cumulatively, Indonesia has lost 30% of its mangrove forests between 1980 and 2005; this is equivalent to an annual deforestation rate of 1.24% (Murdiyarso et al. 2015). The destruction of mangroves is usually related to human population density (Donato et al. 2011).

The continued decline in mangrove forests due to various anthropogenic activities in various regions in Indonesia has increased the concern of the stakeholders in mangrove forests conservation field. Various efforts have been made by these stakeholders, including by the government. The Forestry Department has been, is, and will carry out activities in the form of technical operational activities, both the field and in the concept (Forestry Department 2003).

In 2007, Forestry Department of West Java Province performed a rehabilitation program of mangrove forest in a total of 750 ha areas (outside the forest area) spread in Indramayu, Ciamis, and Subang Districts. The program was implemented by using a green belt and ditch pond pattern. To achieve the expected goals, the implementation of such activity need to be monitored and evaluated routinely (Forestry Department of West Java Province 2008). In the implementation, monitoring efforts of mangroves rehabilitation program are less intensive because of a direct monitoring over a large area requires an enormous number of human resources, funds, and time.

Thus, a different approach is needed. The most possible approach is to conduct the monitoring effort by using remote sensing technology.

Remote Sensing (RS) refers to obtaining information about objects or areas at the Earth's surface without being in direct contact. Remote sensing uses a part or several parts of the electromagnetic spectrum. It records the electromagnetic energy reflected or emitted by the earth's surface (Aggarwal 2007). Remote sensing can be performed with limited funds (cost) by using open source software (e.g. GRASS GIS and QGIS) and Satellite images that have been provided for free (e.g. Landsat Programs). Through this study, we want to help the evaluation and the monitoring of mangrove rehabilitation program undertaken by the government and to promote remote sensing as an inexpensive method to perform these activities with reliable results. Several studies, for example, have applied remote sensing technology for monitoring, evaluating, and conserving mangrove ecosystems by Huang et al. (2009), Lee and Yeh (2009), Giri et al (2011), Kuenzer et al. (2011), and Ramdani et al. (2015).

MATERIALS AND METHODS

Study area

Multispectral images of Landsat 4-5 TM (1996), Landsat 7 ETM+ (2006), and Landsat 8 OLI (2016) were collected from the United States Geological Survey (USGS) website (http://earthexplorer.usgs.gov). The multispectral imagery consists of 11 spectral bands for Landsat 8 OLI and 8 spectral bands for Landsat 4-5 TM and Landsat 7 ETM+. The selected imageries were acquired over the Subang and Indramayu Districts of West Java Province, Indonesia (Figure 1).

Procedures

Landsat image pre-processing

The first necessary step to analyze vegetation indices and land use/land cover is to perform image Pre-processing. The Landsat 8 OLI and 7 ETM+ images were geometry-corrected by the U.S Geological Survey (USGS), while the Landsat 4-5 TM was corrected by using the GCP points data collected from USGS (USGS 2013).

Landsat Image Pre-processing means to convert the digital number (DN) values to the surface reflectance (Top of Canopy) values by using a two-step process. This level of data correction is the proper level of correction to perform vegetation indices calculation and land use/land cover analysis (GrassGIS Development Team 2013). The first step is to convert the DN values into radiance values using the Lmin and Lmax spectral radiance scaling factors (USGS 2013). The values are specific to the individual scene and are produced in the image header file (Ramdani et al. 2015). The gain and bias for TOA radiance calibration in the Landsat 4-5 TM and Landsat 7 ETM+ data could be read in the metadata(.MTL) file as "mult" and "add" values that are also similar to Landsat 8 OLI (USGS 2016). The "mult" is a multiplicative rescaling factor, while "add" is an additive rescaling factor for each band (Ramdani et al. 2015).

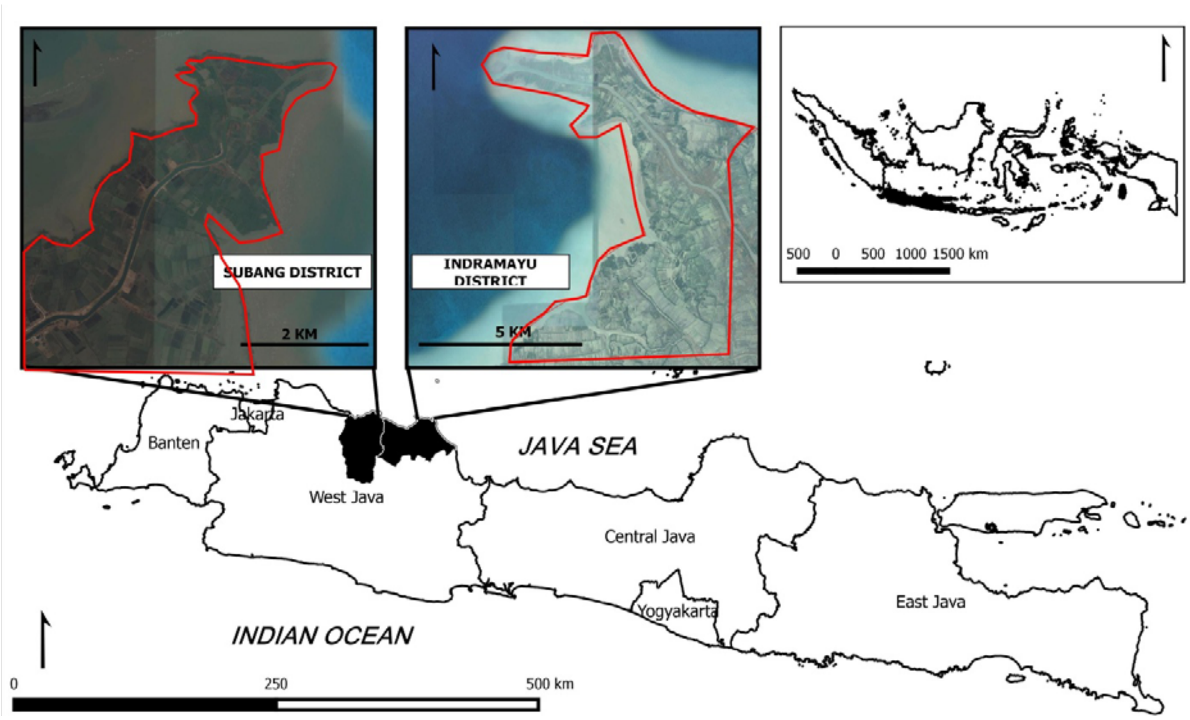

Figure 1. The study areas were located in Cantigi sub-District, Indramayu and Pusakanagara sub-District, Subang, West Java Province, Indonesia. Images were taken from Google Earth. The red polygon represents the area of the program.

The second step is to convert the radiance values into Surface reflectance values using the 6S (Second Simulation of Satellite Signal in the Solar Spectrum) algorithm. The atmospheric correction process is essential when the multi-temporal analysis is conducted (Fichera et al. 2012). The effect of atmosphere can prevent the proper interpretation of the image if it is not taken into account (Martinez et al. 2008; Abrams et al 2009; Hadjimitsis et al. 2010; Srivastava et al. 2014; Hagolle et al. 2015; Raab et al. 2015). The USGS currently provides a higher-level data product which is already converted into surface reflectance. However, to calculate Landsat 4-5 TM, 7 ETM+, and Landsat 8 OLI surface reflectance values the USGS used two different Algorithms, namely: (i) LEDAPS (Landsat Ecosystem Disturbance Adaptive Processing System) for Landsat 4-5 TM and Landsat 7 ETM+. (ii) LaSRC (Landsat Surface Reflectance Code) for Landsat 8 OLI (USGS 2016). Furthermore, a study of the continuity of reflectance data between Landsat-7 ETM and Landsat 8 OLI by Flood (2014) exhibited that there were slight differences in the reflectance measurements of both Series of Landsat. Thus, the standardization of surface reflectance algorithm is essential by using the 6S algorithm. All of the 6S parameter values needed to perform the algorithm were obtained from the USGS (https://landsat.usgs.gov/calibration). After these steps had finished, the pixel values of each scene were atmospherically corrected as surface reflectance.

To convert the radiance values into surface reflectance values in GRASS GIS software, we used the "r.atcorr" tool with the requirement of nine parameters. The nine 6S Parameters required were : (i) Geometrical conditions, (ii) Acquiring date of the image (month, day, decimal hours GMT), (iii) Longitude and latitude in the middle of the image, (iv) Atmospheric model, (v) Aerosol model, (vi) Visibility in Kilometer(s) (Aerosol model concentration), (vii) Mean target elevation above sea level in Kilometer(s), (viii) Sensor height (Sensor on board satellite) in Kilometer(s), and (ix) Selected Sensor band.

NDVI and NDWI

The images that were atmospherically corrected then could be used to perform the NDVI (Normalize Difference Vegetation Index) (Sharma et al. 2009) and NDWI (Normalize Difference Water Index) (Yilmaz et al. 2008) calculation. The purpose of this step is to provide the necessary indices images that will be used as classification factors.

NDVI is a numerical indicator that uses the visible and near-infrared bands of the electromagnetic spectrum. NDVI is adopted to analyze the density of vegetation and also to separate the healthy vegetation and unhealthy or sparse vegetation, (Devadas2008; Genc et al. 2008; Szilárd et al 2016) by the use of density as a base of hypothetical measurement. In the command console of GRASS GIS, the formula to calculate the NDVI is written as follows (equation 1).

r.mapcalc NDVI = 1.0×(NIR – Red)/(NIR + Red) (equation 1)

Where, NIR is stood for Near Infrared channel corresponds to Band 4 (0.77 – 0.90 μm) for Landsat 7 ETM+ and Landsat 4-5 TM, and to Band 5 (0.85 – 0.88 μm) for Landsat 8 OLI. Red channel is a visible wavelength channel at Band 3 (0.63 - 0.69 μm) for TM and ETM+ and at Band 4 (0.63 - 0.68 μm) for OLI images.

NDWI is sensitive to the changes in the water content of vegetation canopies. It is considered as an independent vegetation index that was developed to delineate vegetation water content features and to enhance their presence in remotely sensed digital imagery (Alsaaideh et al. 2013; Ramdani et al. 2015). In the command console of GRASS GIS, the formula to calculate the NDWI is written as follows (equation 2). Every formula that contains and will result in float values calculated in GRASS GIS needs to be multiplied by 1.0 to ensure that the results of the data are in the same float values. Multiplying the equation by 1.0 will give GRASS GIS information it needed to handle or operate the equation in the manner of floating value. Thus, the result will come out as a float value rather than an integer value if such information is not included in the equation (GrassGIS Development Team 2016).

r.mapcalc NDWI = 1.0×(Green −SWIR)/(Green + SWIR) (equation 2)

Where, SWIR (Short Wavelength Infrared) is the reflectance in a short wavelength Infrared and corresponds to Band 5 (1.55 – 1.75 μm) for Landsat 7 ETM+ and Landsat 4-5 TM and to Band 6 (1.57 – 1.65 μm) for Landsat 8 OLI.

RGB composite

RGB (Red-Green-Blue) composite was performed by composing three different band channels to produce a new image that shows the different nature of land surface color based on its response to an electromagnetic impulse from the sun (Xie et al. 2008). The red channel in RGB composite was made by using the Blue Band in Landsat 7 ETM+ and Landsat 4-5 TM, while in Landsat 8 OLI the deep blue coastal band was used. NDVI image was used as the Green channel, and NDWI image as the Blue channel (Ramdani et al. 2015). In the command console of GRASS GIS, the formula to calculate the RGB composite is written as follows (equation 3). Because of the wide distribution of fish pond in the study areas, NDWI was then used to accurately differentiate the waterbody and non-waterbody in those areas since the utilization of green and NIR wavelengths are advisable to monitor water content in water bodies (Li et al. 2013; Koet al. 2015; Mishra and Rama 2015; Gulcan and Mehmet 2016; Yun et al. 2016). Several studies by Xu (2006), Li et al. (2013), Szabo et al. (2016), and Gao et al. (2016) have been conducted in an attempt to utilize the NDWI as a tool to extract the waterbody content in order to map the land surface water with acceptable results. The NDVI was used to indicate the green vegetation presents in the pixel to classify vegetated and non-vegetated areas (Verrelst et al. 2008; Bhandari et al. 2012; Pujiono et al 2013).

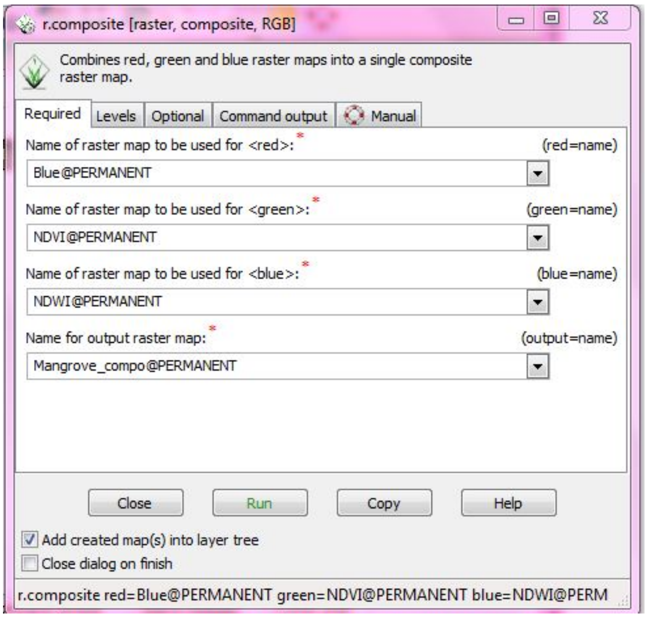

Figure 2. Screenshot of the r.composite tool in Grass GIS ver. 7.0.2.

r.composite r = Blue g = NDVI b = NDWI output = Mangrove_compo (equation 3)

Where :
r = Red Channel
g = Green Channel
b = Blue Channel

Image fusion

Since Landsat 4-5 TM does not has a panchromatic band, the image fusion technique was performed only on Landsat 7 ETM+ and Landsat 8 OLI. An image fusion technique was conducted using the panchromatic band of Landsat 7 ETM+ and Landsat 8 OLI and the RGB image. This technique was performed to enhance the image resolution for a better visual interpretation and to enhance the classification result by fusing the high spatial resolution of the panchromatic image with the multispectral content of multiband images (RGB image) into a single band (Cetin and Musaoglu 2009; Butt et al. 2015; Muhsin and Salih 2015). Several examples of the study conducted by Han et al. (2008), Sarup and Singhai (2011), and Yuhendra et al. (2011) have illustrated the advancement utilization of image fusion with reliable results. Landsat 8 OLI stores values as "DN" from zero to 65,535. Thus, we need an additional step to rescale it into zero to 255 to get the same acceptable color-balanced composite image as the Landsat 7 ETM+ after pan-sharpening (Ramdani et al. 2015). Rescaling those values can be done using the "r.rescale" expression on GRASS GIS command console (equation 4). The Brovey spectral sharpening technique was used in this study using the "i.pansharpen" expression in GRASS GIS software (equation 5).

r.rescale in = B(i)_DNs from = 0,65535 out = B(i)_DNs_255 to = 0,255 (equation 4)

i.pansharpen equation : output previx =

$$\frac{ms1}{ms1 + ms2 + ms3} \text{ x } pan \qquad \text{(equation 5)}$$

Where,
ms1 = Name of input raster map (Green: B2).
ms2 = Name of input raster map (NIR: B4).
ms3 = Name of input raster map (MIR: B5).
Pan = Name of input raster map (Panchromatic: B8).

Output prefix = Name for output raster map prefix (e.g. "fusedimage").
in = The name of the raster image to be rescaled.
Out = The resulting raster map name.
From = min, max (the input data range to be rescaled).
To = min,max (the output data range).

Image classification

Image classification was performed on the fused images. To extract the mangrove forest area from the images, we used a maximum likelihood decision rule method with two classes that were defined for mangrove forests map: mangrove forest and non-mangrove forest (e.g. built-up area, fishpond, and water).

Generating supervised classification map using the maximum likelihood method can be conducted after creating training area. Training area represents the spectral information of each land use/land cover class (Perumal and Bhaskaran 2010; Ahmad 2012). A vector layer map has to be created to the layer manager before training areas can be digitized. The process is available from the Graphical User Interface (GUI) of GRASS GIS by choosing "develop vector map" in the "vector" menu tab and then click "create vector map". We created 100 training areas for each of fused image. Fifty training areas for every land cover class (mangrove forest and non-mangrove forest) were evenly distributed and mixed pixels were avoided carefully since the selection of training area can significantly influence the performance of image classification algorithm (Kavzoglu and Yildiz 2011; Colditz 2015). The vector training area then must be converted into raster format using the "v.to.rast" expression (equation 6). To select all relevant bands (blue band of Landsat 4-5 TM and Landsat 7 ETM+, a deep blue coastal band of Landsat 8 OLI, NDVI images, and NDWI images) of raster images we used the "i.group" expression (equation 7). To generate statistics from the training area, the "i.gensig" expression (Equation 8) was used. The inputs into the "i.gensig" for the creation of signature statistics are the training area images in raster format, which its format conversion has been performed priory.

The maximum classification likelihood algorithm was performed using the "i.maxlik" expression (equation 9) in GRASS GIS. The results were then converted into vector format using the "r.to.vect" expression (equation 10). The final analysis and cartography design were then performed using QuantumGIS software ver. 2.16.2.

v.to.rast input = training _ vector output = training _ raster (equation 6)
i.group group = Landsat7 _ group subgroup = Landsat7 _ subgroup input = B1,NDVI,NDWI (equation 7)

i.gensigtrainingmap= training _ raster group = Landsat7 _ group subgroup = Landsat7 _ subgroup signaturefile= Landsat7 _ signature (equation 8)

i.maxlik group = Landsat7 _ group subgroup = Landsat7 _ subgroup signaturefile= Landsat7 _ signature class = mangrove _ class7 (equation 9)

r.to.vect -s input = mangrove _ class7 output = mangrove _ class7 feature = area (equation 10)

Field work and accuracy assessment

Field work was carried out in 2 villages from 2 districts namely: (i) Cangkring Village, Cantigi Sub-District, Indramayu. (ii) Patimban Village, Pusakanagara Sub-District, Subang. Field data were collected using Garmin Oregon 550 GPS. For accuracy assessment, Google Earth Imagery was used to help visual interpretation from above the ground. We transformed the image of study area taken from Google Earth into KML format to be imported into the GPS so we are able to performed landcover validation. Two hundred validation points were selected randomly for each study area. The Google Earth image was also used to assist the selection of those validation points so that all of the points were distributed evenly between two land cover classes (mangrove and non-mangrove class). Several points from each village were randomly selected to be validated directly in the field (Hansen and Loveland 2012).

Accuracy assessment calculation was performed by generating a kappa value (Liu et al. 2007; Mas 2012; Ramdani et al. 2015). To generate a kappa value we need to import shapefile data of the ground truth and the classified map (GrassGIS Development Team 2016) into GRASS GIS with "v.in.ogr" command (equation 11), and then convert it again to a raster with "v.to.rast" command (equation 12). We then employed the "r.kappa" command (equation 13) in GRASS GIS command console.

v.in.ogrdsn /home / user / shape _ data layer survey _ data = output = survey _ area
v.in.ogr input=/home/user/shape_data/test_shape.shp output=grass_map (equation 11)

v.to.rast input = survey _ area output = survey _ area (equation 12)

r.kappa classification = mangrove _ class7 reference = survey _ area output = result _ kappa (equation 13)

Where,
layer = Name for input shapefile vector data.
input = Name for input vector map.
output = Name for output vector/raster map.
classification = Name of raster map containing classification result.
reference = Name of raster map containing reference classes.
output = Name for output file containing error matrix and kappa.

RESULTS AND DISCUSSION

RGB color composite and supervised classification using Maximum Likelihood decision rule

RGB (Red-Green-Blue) color composite was produced by using the Blue Band (Landsat 5 TM and Landsat 7 ETM+) and the deep blue coastal in Landsat 8 OLI as red channel, NDVI as Green channel, and NDWI as Blue channel. This combination will produce an image that highlights the striking differences of mangrove forests among another landcover classes.

Maximum likelihood decision rule is a classification tool that considers both the variances and co-variances of the class signatures when assigning each pixel to one of the classes represented in the signature file (Myint et al. 2014; Srivastava et al. 2014) which was made from training area. Therefore, the training area needs to be carefully selected; otherwise, the classification result may introduce error (Ramdani et al 2015). Maximum likelihood utilizes the class signature as a representative means and variance values of each land cover class which are then used to estimate the probabilities. Maximum likelihood decision rule considers not only the mean or average values in assigning classification, but also the variability of the brightness values of each class (Campbell 2011).

Mangrove forest change detection

Mangrove forest change analysis in this study is used to measure the successfulness of mangrove forest plantation program performed by the Forestry Department of West Java in 2007. In addition, this study also measures the mangrove forest change before the program performed. Therefore, we can present a quantitative measurement why such a program was needed.

After overlaying the mangrove forest extraction from classification result in 1996 with the one from 2006 also overlaying the mangrove forest extraction in 2006 with the one from 2016, clearly we can see the changes in the mangrove forest area before and after the program performed.

The kappa analysis and subsequent accuracy of the classification using RGB composite color are presented in Table 1. The kappa statistic of 0.90 provides strong confidence to the results of this study (Gwet 2008; Foody 2009; McHugh 2012).

Table 1. Classification accuracy of Landsat 8 OLI

Class/Region	Water (%)	Mangrove (%)	Fishpond (%)
Water	97.00	0.00	6.00
Mangrove	0.00	97.00	0.00
Fishpond	1.00	0.00	93.00
Overall Kappa = 0.90			
Overall classification accuracy = 93.02%			

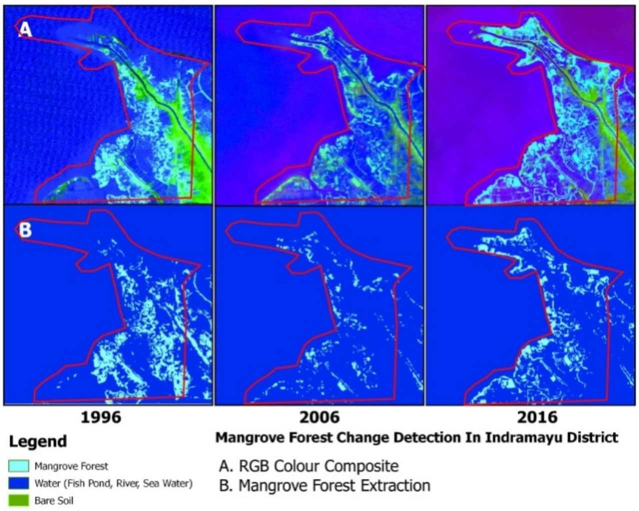

Figure 3. RGB color composite and classification results of mangrove forests in Indramayu District. Group A (from left to right) is the RGB color composite that shows the different color for different types of land surface. Group B (from left to right) shows the Mangrove forests extraction derived from the supervised classification method. The red polygon represents the area of the program.

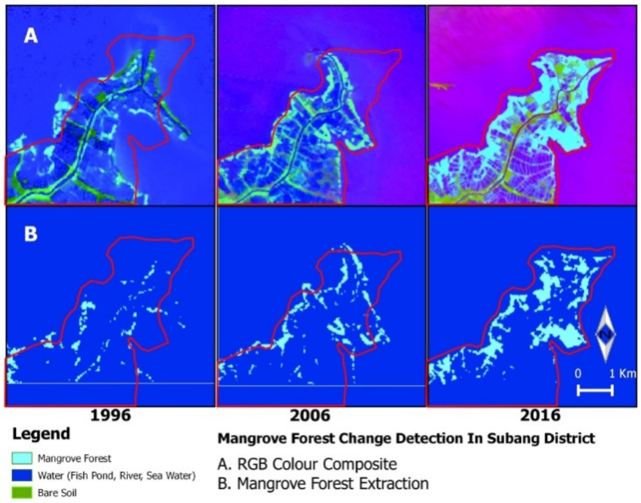

Figure 4. RGB color composite and classification results of mangrove forests in Subang District. Group A shows the RGB color composite that shows a different color for different types of land surface. Group B shows the Mangrove forests extraction derived from a supervised classification method. The red polygon represents the area of the program.

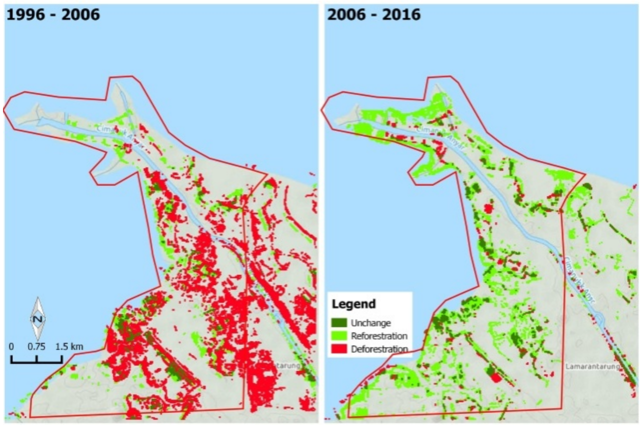

Figure 5. The mangrove forest change detection in Indramayu District derived from the classification method. The year 1996-2006 shows the change before the mangrove forest plantation program was performed in 2007 and the year 2006-2016 shows the change in mangrove forests after the program performed. The red polygon represents the area of the program.

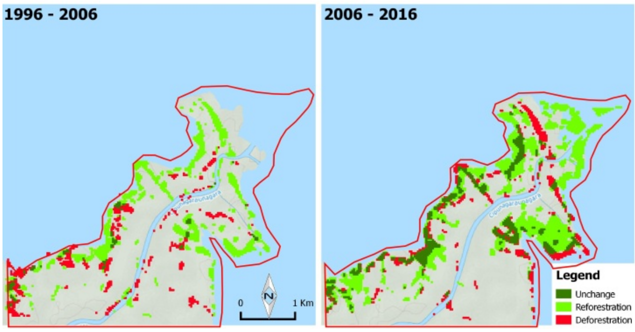

Figure 6. The mangrove forest change detection in Subang District derived from the classification method. The year 1996-2006 shows the change before the mangrove forest plantation program was performed in 2007 and the year 2006-2016 shows the change in mangrove forests after the program performed. The red polygon represents the area of the program.The red polygon represents the area of the program.

Discussion

Mangrove forest change detection over the ten-years period before the program performed in Indramayu was conducted to analyze the general description about why such a program was needed. Figure 3 illustrates the enormous decline in mangrove forest area due to the expansion of fishpond and salt pond activities, as shown in the figure where the sky blue color of mangrove forest declined in conjunction with the increased of the dark blue color of water that found in the fish pond. The quantification of the mangrove forest declining is presented in Table 2. This change was also detected by the Forestry Department; therefore, the mangrove forest plantation program in 2007 was initiated. The mangrove forest plantation program in 2007 was conducted in a total of 400 ha area in Cangkring Village, Cantigi Sub-District, Indramayu. The program was performed with the help of the community since they are well-informed about the ecological advantage of mangrove forest (Forestry Department 2013).

Mangrove forest change detection in the same period of time before the program performed in Subang District shows a different pattern from the result shown in Indramayu. From 1996 to 2006, there was a significant increase in mangrove forest area due to the wide area of abandoned fishpond that remains unused; therefore, it occupied by the mangroves (Figure 5 and Table 3). Lots of fishponds were abandoned as the sudden increase of sea water level flooded their fishpond and released their fishes into the ocean. The farmers then have no more fund to continue their business, so they prefer to search opportunity in another field of business (Forestry Department 2008).

The after-program mangrove forest change detection in the applied area of program in Indramayu shows an increasing area of mangrove forest (Figure 3 and Table 2). The increasing of mangrove forest area at approximately 17.8% $year^{-1}$ indicates the successfulness of the program. The successfulness of the program also detected in the applied area of program in Subang District by the increasing of approximately 16.3% $year^{-1}$ of mangrove forests area. All of these achievements were due to the community participation in rehabilitation, conservation, and management of mangrove forest through the program. However, the community also asked the government to accommodate their need of income from aquaculture activities by increasing their business knowledge through technical training and supporting of seaweed seedlings to diversify the aquaculture activities. In addition, They also demand a clear policy to protect both the sustainable of mangrove forest and the sustainable of their income from aquaculture activities.

Another approach to accommodate those purposes is to re-introduce a system that combines the fishpond (for fish farming and/or shrimp) with mangrove trees in the pond, called silvofishery (Pujiono et al. 2013). In Indonesia, a silvofishery system has been applied since the early 1990s (Wetland International-The Green Coast Project 2006). The Southeast Asian Fisheries Development Center (SEAFDEC) stated that the model of silvofishery consists of a ratio of 60–80% mangroves and 20–40% pond canal for aquaculture. This system has a great chance to be rejected by the people if the re-introduction does not conduct properly. People will assume that the silvofishery system will reduce their fish productivity because of the high proportion of land that must be occupied by mangrove plants. They will apparently need some proof and warranty that silvofishery system will not reduce their productivity. To answer this question, the study conducted by Kupang Forest Research Institute in 2009 found that the fish weight in the silvofishery system is greater than that of the traditional fishpond (Pujiono et al. 2013). In addition, during the first two years of observation, the growth rate of mangrove species (*Rhizophora mucronata* Lam.) reached 16.01 cm $year^{-1}$ and the growth rate of diameter reached 1.02 cm $year^{-1}$ (Njurumana et al. 2010). Another study, focusing on assessing the advantage of silvofishery system, was conducted in Vietnam in a two-years period of time by Food and Agriculture Organization of the United Nations (FAO). FAO reported an increasing of the shrimp productivity by 10% $year^{-1}$ after the silvofishery program was initiated. This implementation of silvofishery system in Cha Mau Province, Vietnam, project will be held for the next 20 years. Thus, the silvofishery system has been proofed to be a suitable method to be implemented as an addition program of mangrove rehabilitation.

Table 2. Temporal changes of mangrove area in applied area of program in Indramayu District, West Java Province, Indonesia

Year	Area (ha)	Changes (%)
1996	1060.83	0.00
2006	258.75	-75.6
2016	719.46	+174.2

Table 3. Temporal changes of mangrove forest area in applied area of program in Subang District, West Java Province, Indonesia

Year	Area (ha)	Changes (%)
1996	60.93	0.00
2006	123.12	+102.1
2016	336.47	+173.3

The increasing of mangrove forest areas both in Indramayu and Subang Districts indicates that the main purpose of the mangrove plantation program has been achieved. The sustainability of the mangrove forest in these areas is another goal that can be ensured by maintaining the positive growth rate of mangrove forest. To achieve this goal, the government must not abandon the participation of the community. The community will gladly participate in such a program if they can gain some profits in return. Thus, the idea of ensuring sustainability of both the mangrove forests and the income from aquaculture activities must become a long-term program of the government. To monitor both the short and long-term mangrove rehabilitation program, remote sensing is proposed to be used widely to become such an initial step to collect fast, robust, and reliable data.

This study also tried to highlight the importance of freely available geospatial software such as GRASS GIS and QGIS software and satellite images that are freely available in the public domain such as Landsat data. Several studies have been conducted by implementing the inexpensive method of remote sensing to remotely observe the change and the conversion of mangrove forest area; for example, the application of Landsat image to assess the decreased of mangrove forest area in Al-Dakhira, The State of Qatar (Balakrishnan 2012). This study presented that the application of an inexpensive method of remote sensing is extremely useful to understand the coastal habitats, especially mangroves.

The application of Landsat images and open source software also implemented in the study of mangrove mapping and change detection in HaiPhong City, Vietnam (Dat-Pham 2015). This study highlights the mangrove forests declining throughout the year 1989 to 2013 with the overall accuracy of 83% and the Kappa coefficient of 0.81. In Indonesia, Ramdani et al. (2015) also promote the use of inexpensive method of remote sensing to be used widely in an attempt to help monitor the mangrove forest areas in Indonesia without encumbering the government financially. In addition, this study also pursued the same goals with the specification in evaluating and monitoring the mangrove plantation program held by the government.

ACKNOWLEDGEMENTS

The authors gladly thank the Ministry of Forestry for several data which have been provided to help this study and the Bird Conservation Society (BICONS) for the support in providing tools the authors needed. The authors by this declare that there is no conflict of interest.

REFERENCES

Abrams M, Feidas H, Arai K. 2009. Comparison of atmospheric correction methods using ASTER data for the area of Crete, Greece. Int J Remote Sens 31: 6347-6385.

Ahmad A. 2012. Analysis of maximum likelihood classification on multispectral data. Appl Math Sci 6: 6425-6436.

Alongi DM. 2008. Mangrove forests: Resilience, protection from tsunamis and responses to global climate change. Est Coast Shelf Sci 76: 1-13.

Alsaaideh B, Al-Hanbali A, Tateishi R, Kobayashi T, Hoan NT. 2013. Mangrove forest mapping in the southern part of Japan using Landsat ETM+ with DEM. J Geo Info Sys 5: 369-377.

Balakrishnan P. 2012. Application of Remote Sensing for mangrove mapping: a case study of Al-Dhakira, the State of Qatar. J Earth SciEng 2: 602-612.

Barbier EB, Hacker SD, Kennedy C, Evamaria WK, Stier AC, Silliman BR. 2011. The value of estuarine and coastal ecosystem services. EcolMonogr 81: 169-193.

Bhandari AK, Kumar A, Singh GK. 2012. Feature extraction using Normalized Difference Vegetation Index (NDVI): a case study of Jabalpur City. Proc Tech 6: 612-621.

Butt A, Shabbir R, Ahmad SS, Aziz N. 2015. Land use change mapping and analysis using Remote sensing and GIS: a case study of Simly Watershed, Islamabad, Pakistan. J Remote SensSpSci 18: 251-259.

Cetin M, Musaoglu N. 2009. Merging hyperspectral and panchromatic image data: qualitative and quantitative analysis. Int J Remote Sens 30: 1779-1804.

Campbell JB, Randolph H, Wyne. 2011. Introduction to Remote Sensing, 5th ed. Guilford Press, New York.

Colditz RR. 2015. An evolution of different training sample allocation schemes for discrete and continuous land cover classification using decision tree-based algorithms. Remote Sens 7: 9655-9681.

Dat-Pham T, Kunihiko Y. 2015. Mangrove mapping and change detection using multi-temporal Landsat imagery in Hai Phong city, Vietnam. In: Arikawa M, Tsou MH (eds) Proceedings of The International Symposium on Cartography in Internet and Ubiquitous Environments. Tokyo University, Tokyo, 17th - 19th March 2015.

Devadas R, Lamb DW, Simpfendorfer S, Backhouse D. 2008. Evaluating ten spectral vegetation indices for identifying rust infection in individual wheat leaves. PrecisAgric 10: 459-470.

Donato DC, Kauffman JB, Murdiyaso D, Kurnianto S, Stidham M, Kanninen M. 2011. Mangroves among the most carbon-rich forests in the tropics. Nat Geo 4: 293-297.

Fichera CR, Modica G, Polling M. 2012. Land cover classification and change-detection analysis using multi-temporal Remote sensed imagery and landscape metrics. Eur J Remote Sens 45: 1-18.

Flood N. 2014. Continuity of reflectance data between Landsat-7 ETM+ and Landsat-8 OLI for both top-of-atmosphere and surface reflectance: a study in the Australian landscape. Mdpi Remote Sens J 6: 185-201.

Food and Agriculture Organization of the United Nations (FAO). 2007. The world's mangroves 1980–2005: A thematic study prepared in the framework of the global forest resources assessment. FAO Forestry Paper Publisher, Rome.

Foody GM. 2009. Classification accuracy comparison: hypothesis tests and the use of confidence intervals in evaluations of difference, equivalence and non-inferiority. Remote Sens Environ 113: 1658-1663.

Forestry Department. 2013. Mangrove forest policy in Indonesia. Forestry Department. www.dephut.go.id [Indonesian]

Gao H, Wang L, Jing J, Xu. 2016. An effective modified water extraction method for Landsat-8 OLI imagery of mountainous plateau regions. Earth Environ Sci 42: 257-266.

Genc H, Genc L, Turhan H, Smith SE, Nation JL. 2008. Vegetation indices as indicators of damage by the sunn pest (Hemiptera: Scutellaridae) to field grown wheat. Afr J Biotech 7: 357-371.

Giri C, Ochieng E, Tieszen LL, Zhu Z, Singh A, Loveland T, Masek T, Duke N. 2011. Status and distribution of mangrove forests of the world using earth observation satellite data. Glob EcolBiogeogr 20: 154–159.

GrassGIS Development Team. 2016. GRASS GIS manual: r.mapcalc. https://grass.osgeo.org/grass64/manuals/r.mapcalc.html

Gulcan S, Mehmet O. 2016. Water body extraction and change detection using time series: a case study from Lake Burdur, Turkey. J TaibahUnivSci 9: 126-137.

Gwet KL. 2008. Computing inter-rater reliability and its variance in the presence of high agreement. Brit J Math Stat Psy 61: 29-48.

Hadjimitsis DG, Papadavid G, Agapion A, Themistocleous, Retalis A, Michaelides S, Chrysoulakis N, Toulios, Clayton C. 2010. Atmospheric correction for satellite Remote sensed data intended for agricultural applications: impact on vegetation indices. Nat Hazards Earth Sys Sci 10: 89-95.

Hagolle O, Huc M, Pascual DV, Dedieu G. 2015. A multi-temporal and multi-spectral method to estimate aerosol optical thickness over land, for the atmospheric correction of FormoSat-2, LandSat, VENμS and Sentinel-2 Images. Remote Sens 7: 2668-2691.

Han SS, Lia HT, Gua HY. 2008. The study on image fusion for high spatial resolution Remote sensing images. Remote Sens Spat Inf Sci 37: 1159–1164.

Hansen MC, Loveland TR. 2012. A review of large area monitoring of land cover change using Landsat data. Remote Sens Environ 122: 66-74.

Huang X, Zhang L, Wang L. 2009. Evaluation of morphological texture features for mangrove forest mapping and species discrimination using multispectral IKONOS imagery. IEEE Geo Remote Sens 6: 393-397.

Hussain SA, Badola R. 2010. Valuing mangrove benefits: contribution of mangrove forests to local livelihoods in Bhitarkanika Conservation Area, East Coast of India. Wetlands EcolManag 18: 321-331.

Kavzoglu T, Yildiz M. 2014. Parameter-based performance analysis of object-based image analysis using aerial and Quickbird-2 images. Remote Sens Spat InfSci 7: 31-37.

Ko CB, Kim HH, Nam JY. 2015. Classification of potential water bodies using Landsat 8 OLI and a combination of two boosted random forest classifiers. Sens 15: 13763-1377.

Kuenzer C, Bluemel A, Gebhardt S, Quoc VT, Dech S. 2011. Remote sensing of mangrove ecosystem: a review. Remote Sens 5: 878-923.

Lee TM, Yeh HC. 2009. Applying Remote sensing techniques to monitor shifting wetlands vegetation: A case study of Danshui River estuary mangrove communities, Taiwan. Ecol Eng 35: 487-496.

Li W, Zhiqiang D, Feng L, Dongbo Z, Hailei W, Yuanmiao G, Bingyu S, Xiaoming Z. 2013. A comparison of land surface water mapping using the Normalized Difference Water Index from TM, ETM+ and OLI. Remote Sens 5: 5530-5549.

Liu C, Frazier P, Kumar L. 2007. Comparative assessment of the measures of thematic classification accuracy. Remote Sens Environ 107: 606-616.

Martinez L, Caselles V, Pala V, Valor E. 2008. Emissivity errors in the vegetation cover method caused by the lack of atmospheric correction. Int J Remote Sens 29: 1825-1832.

Mas JF. 2012. Monitoring land-cover changes: a comparison of change detection technique. Int J Remote Sens 20: 139-152.

McHugh ML. 2012. Inter-rater reliability: the kappa statistic. Biochem Med 22: 276-282.

Mishra K, Rama CP. 2015. Automatic extraction of water bodies from Landsat imagery using perceptron model. J CompEnviron Sci 9: 2314-8292.

Muhsin IJ, Salih KH. 2015. Enhancement and quality assessment of multi-spectral image using different fusion methods. Iraqi J Sci 56: 257-264.

Murdiyarso D, Joko P, Boone K, Matthew WW, Sigit DS, Daniel CD, Solichin M, Haruni K, Sartji T, Sofyan K. 2015. The potential of Indonesian mangrove forests for global climate change mitigation. Nat ClimCh 5: 1089–1092

Myint SW, Gober P, Brazel A, Clarke SG, Weng Q. 2011. Per-pixel vs object-based classification of urban land cover extraction using high spatial resolution imagery. Remote Sens Environ 115: 1145-1161.

Njurumana G, Pujiono E, Soenarno. 2010. Mangrove forest rehabilitation through silvofishery. In: Rimbawan A, Febrianto F, Komar ET (eds).

Proceedings International Seminar of Research on Plantation Forests: Challenges and Opportunities. CIFOR, Bogor, 5-6 November 2010.

Perumal K, Bhaskaran R. 2010. Supervised classification performance of multispectral images. J Comp 2: 376-389.

Pujiono E, Kwak DA, Lee WK, Sulistyanto, Kim SR, Lee JY, Lee SH, Park T, Kim MI. 2013. RGB-NDVI Color composites for monitoring the change in mangrove area at Maubesi Nature Reserve, Indonesia. Sci Tech 9: 171-179.

Raab C, Barrett B, Cawkwell F, Green S. 2015. Evaluation of multi-temporal and multi-sensor atmospheric correction strategies for land-cover accounting and monitoring in Ireland. Remote Sens 6: 784-793.

Ramdani F. Rahman S. Setiani P. 2015. Inexpensive method to assess mangroves forest through the use of open source software and data available freely in public domain. J Geo Inf Sys 7: 43-57.

Sharma AR, Badarinath KVS, Roy PS. 2009. Comparison of ground reflectance measurement with satellite derived atmospherically corrected reflectance: a case study over semi-arid landscape. AdvSp Res 43: 56-64.

Srivastava, Han D, Miguel A, Ramirez R, Bray M, Islam T, Gupta M, Dai Q. 2014. Estimation of land surface temperature from atmospherically corrected LANDSAT TM image using 6S and NCEP global reanalysis product. Environ Earth Sci 72: 5183-5196.

Srivastava, Prashant K., Dawei H, Miguel A. Rico R, Michaela B, Tanvir I. 2012. Selection of classification techniques for land use/land cover change investigation. Adv Sp Re 50: 736-747.

Szilárd S, Zoltán G, Boglárka B. 2016. Specific features of NDVI, NDWI And MNDWI as reflected in land cover categories. Landsc Environ 10: 194-202.

United States Geological Survey (USGS). 2013. Using the USGS Landsat 8 product. NASA. www.Landsat.usgs.gov

United States Geological Survey (USGS). 2016. Landsat surface reflectance higher-level data products. NASA. www.landsat.usgs.gov

United States Geological Survey (USGS). 2016. How is radiance calculated. NASA. www.Landsat.usgs.gov

Verrelst J, Schaepman ME, Koetz B, Kneubuhler M. 2008. Angular sensitivity analysis of vegetation indices derived from CHRIS/PROBA data. Remote Sens Environ 112: 2341-2353.

Wetlands International-The Green Coast Project. 2006. Understanding linkages of mangrove forest and livelihood: a best practice model in Lam Ujong Village, Aceh Besar District. Wetlands. www.wetlands.org

Yilmaz MT, Hunt ER, Jackson TJ. 2008. Remote sensing of vegetation water content from equivalent water thickness using satellite imagery. Remote Sens Environ 112: 2514-2522.

Yun D, Yihang Z, Feng L, Qunning W, Wenbo L, Xiaodong L. 2016. Water bodies' mapping from Sentinel-2 imagery with Modified Normalized Difference Water Index at 10-m spatial resolution produced by sharpening the SWIR band. Remote Sens 8: 136-147.

Xie Y, Sha Z, Yu M. 2008. Remote sensing imagery in vegetation mapping: a review. J Plant Ecol: 9-23.